Asymmetric Growth of Silver Citrate Compounds by Mechanical Stirring and Their Enhanced Antimicrobial Activity

Heung Ju Jang,[†] Hyosuk Yun,[‡] Se-Woung Oh,[§] Byoung-Gue Jung,[†] Chul Won Lee,[‡,*] and Jong Kuk Lim[†,*]

[†]*Department of Chemistry, Chosun University, Gwangju 61452, Korea. *E-mail: jklim@chosun.ac.kr*
[‡]*Department of Chemistry, Chonnam National University, Gwangju 61186, Korea. *E-mail: cwlee@jnu.ac.kr*
[§]*Department of Chemistry, Mokpo National University, Mokpo 58554, Korea*
Received April 21, 2017, Accepted July 10, 2017, Published online August 24, 2017

The development of a new class of antibiotics is urgently needed, because antibiotic resistance became a serious problem in the pharmaceutical and medical fields. Recently, silver compounds, composed of silver and organic molecules, have been developed as effective antimicrobial agents. For instance, silver citrate ($Ag_3C_6H_5O_7$; Ag-Cit) compounds prepared in the form of precipitates can exhibit a strong antimicrobial activity. Ag-Cit compounds were easily prepared in the mixture of $AgNO_3$ and trisodium citrate dihydrate ($C_6H_5Na_3O_7{\cdot}2H_2O$) solutions. Herein, we demonstrated that simple mechanical stirring significantly changed the morphology (shape and size) of Ag-Cit from bulk (bulk Ag-Cit) to rod-like nanostructures (Ag-Cit nanorods). Ag-Cit nanorods exhibited antimicrobial activity stronger than that of bulk Ag-Cit against both Gram-negative and -positive bacteria. These data indicate that the bactericidal activity of Ag-Cit compounds is dependent on their morphology and will provide valuable information for the development of antimicrobial materials based on Ag-Cit compounds.

Keywords: Antimicrobial activity, Silver citrate compound, Asymmetric growth, Nanorods, Mechanical stirring

Introduction

From the pre-Christ era, ancient people (*e.g.*, Egyptians) used silver (Ag) vessels for storing water or other liquids.[1,2] Although they lacked knowledge of the germicidal effect of Ag, from their experiences, they knew that Ag vessels could prevent water from spoiling, and just empirically used them for storage. It was not until the late 1800s that Ravelin and Naegeli undertook scientific investigation of the biocidal effect of Ag. They found that low concentration of silver ions (Ag^+) from metallic Ag exhibits antimicrobial activity.[3,4] Since then, silver salts (*e.g.*, $AgNO_3$) and compounds (*e.g.*, silver sulfadiazine) have been used in clinical practice as therapeutic compounds.[5,6] Even though antimicrobial activity of Ag^+ has been confirmed in the clinical field for many decades, its mechanism of action is still not clear, and is controversial. The most generally accepted mechanism is that Ag^+ interacts with thiol (−SH) groups of amino acid residues in proteins. Ag^+ easily forms chemical bonds with thiol groups of cysteine, and can inactivate proteins or enzymes containing a cysteine residue, resulting in malfunction of ion pumps in cell membranes or generation of reactive oxygen species.[7–9]

In addition to silver, various organic molecules, such as mafenide and citrate, are known to exhibit antimicrobial activity. Because most of the microorganisms are fastidious and require appropriate environmental conditions for prolonged survival and growth, altering the environmental condition can influence or inhibit their growth. For example, one effective way to limit the growth of microorganisms is by decreasing the pH values lower than the tolerance limit for survival or growth of microorganisms. Hence, most of the acids, such as citric acid and malic acid, can show antimicrobial activity. Sodium citrate, which is an acid–base pair of citric acid, can also exhibit antimicrobial activity, but its mechanism of action is quite different from that of citric acid. It is believed that citrate plays a key role in germicidal effect of sodium citrate, because citrate can form a chelate compound with ions essential for growth of microorganisms. Several scientific papers have reported the inhibitory effect of citrate.[10–12]

Because many organic molecules also have antimicrobial activity, a synergistic effect, owing to combinatorial use of Ag^+ ions and biocidal organic molecules, can be expected. Silver sulfadiazine (SSD) is a representative combinatorial compound, which is prepared by combining Ag^+ and a derivative of mafenide, which is an antimicrobial organic molecule. SSD has been generally used as a topical cream for patients with burn wounds in clinical practice. Due to the same reason, one can also expect that silver citrate compounds (Ag-Cit) will exhibit a synergistic antimicrobial effect. As an example, recently, it has been reported that

the precipitates of Ag-Cit are dissolved into citric acid solution as a complex form $[Ag_3(C_6H_5O_7)^{n+1}]^{3n-}$, and such complexes exhibit strong antimicrobial activity.[13] This type of Ag-Cit complex is already commercially available.[14–16]

In addition to the combinatorial use of different biocidal materials, size of the material is also an important factor determining their antimicrobial activity. As the concentration of ions of biocidal materials (Ag^+ or citrate ion), released from Ag-Cit compounds, is proportional to the contact surface area of Ag-Cit compounds with the environment, it can be anticipated that smaller Ag-Cit compounds would have a stronger antimicrobial activity than that of larger Ag-Cit compounds.[17–20] To decrease the size of Ag-Cit compounds and increase their contact surface area, we introduced mechanical stirring, which can generate more nuclei under same volume condition, resulting in smaller-sized Ag-Cit compounds. When Ag-Cit compounds are prepared with mechanical stirring, it was found that not only their size but also the shape is dramatically changed from bulk to rod-like nanostructure.

The morphology of both the Ag-Cit compounds (bulk Ag-Cit and Ag-Cit nanorods) was characterized by scanning electron microscopy (SEM), and their chemical composition was analyzed using Fourier transform infrared spectroscopy (FT-IR) and X-ray diffractometry (XRD). The antimicrobial activity of both the Ag-Cit compounds was examined against to various bacteria (*Escherichia coli*, *Salmonella typhimurium*, *Pseudomonas aeruginosa*, *Bacillus subtilis*, *Staphylococcus epidermidis*, *and Staphylococcus aureus*) by paper-disc diffusion assay and minimal inhibitory concentration (MIC) was determined. These studies suggest that the antimicrobial activity of Ag-Cit compounds depends on their shape and size, providing valuable information for the development of new antimicrobial agents.

Experimental

Chemicals and Synthesis. Silver nitrate ($AgNO_3$, ≥99.0%, Aldrich, Seoul, Korea) and trisodium citrate dihydrate (TSC, $C_6H_5Na_3O_7{\cdot}2H_2O$, 99.0%, OCI Ltd., Seoul, Korea) were used without any further purification, and highly purified deionized (DI) water (18.2 MΩ cm) generated using QPAK1 (Millipore, Massachusetts, United States) was used for preparing all aqueous solutions. For the synthesis of Ag-Cit precipitates, firstly two aqueous solutions ($AgNO_3$ [0.2 M] and TSC [0.2 M]) were separately prepared at room temperature in different beakers. As soon as they were mixed, white precipitates were formed. The mixed solution containing white precipitate was covered with an aluminum foil, and was divided into two fractions. One batch was stirred at ~340 rpm for 0.5 h at room temperature to synthesize Ag-Cit nanorods, and the other one was not stirred, but placed on an experimental bench without any perturbation for the same period (0.5 h) at room temperature to prepare bulk Ag-Cit.

Characterization. To observe the morphology of Ag-Cit precipitates, the mixed solutions containing Ag-Cit precipitates (bulk Ag-Cit or Ag-Cit nanorods) were drop-casted on an Si wafer, and allowed to dry for several hours. While the solvent was evaporated from the mixed solution on the Si wafer, condensed ions covered the surface of the Ag-Cit precipitates. Because the layer of condensed ions hinders observation of the morphology of Ag-Cit precipitates in SEM, the Ag-Cit precipitates should be washed with DI water several times, after complete drying of the solvent. To increase the conductivity of the sample, platinum was deposited onto the surface of Ag-Cit precipitates at a coating rate of 6 nm/min for 60 s using an ion sputter (E-1030; Hitachi, Tokyo, Japan), and then the morphology of Ag-Cit precipitates (bulk Ag-Cit or Ag-Cit nanorods) was observed by SEM (S-4800; Hitachi, Tokyo, Japan). Composition analysis was performed by FT-IR (Nicolet 6700; Thermo, Massachusetts, United States) using KBr pellet method and XRD (X′pert PRO MPD; Panalytical, Almelo, Netherlands) using Cu Kα radiation.

Paper-Disc Diffusion Method. The paper-disc diffusion assay was used to determine the antibacterial activities of Ag-Cit precipitates (bulk Ag-Cit or Ag-Cit nanorods). Bacteria were initially cultured in Luria-Bertani (LB) media at 37°C for 4 h. A suspension of *E. coli* (KCTC 1682) (50 μL with 1×10^7 colony forming units/mL [CFU/mL]), which were obtained from the Korean Collection for Type Cultures (KCTC) at the Korea Research Institute of Bioscience and Biotechnology, were inoculated on Mueller Hinton agar (MHA) plates. Whatman filter paper discs (4 mm diameter) were placed on the inoculated plates and 20 μL samples (in the concentration range 0–16 μg/mL) were added and allowed to dry for 15 min, after which they were incubated at 37°C for 16 h.

MIC Measurements. The antibacterial activities of the Ag-Cit precipitates (bulk Ag-Cit or Ag-Cit nanorods) were examined in sterile 96-well plate as follows. Aliquots (100 μL) of the cell suspension at 4×10^6 CFU/mL in 1% peptone were added to 100 μL sample solutions (dilutions in 1% peptone). After incubation for 15 h at 37°C, the MIC was determined by visual examination based on the lowest concentration of sample solution in cells with no bacterial growth. Three Gram-negative bacteria (*E. coli* [KCTC 1682], *S. typhimurium* [KCTC 1926], and *P. aeruginosa* [KCTC 1637]) and three Gram-positive bacteria (*B. subtilis* [KCTC 3068], *S. epidermidis* [KCTC 1917], and *S. aureus* [KCTC 1621]) were obtained from KCTC at the Korea Research Institute of Bioscience and Biotechnology.

Results and Discussion

Ag-Cit ($Ag_3C_6H_5O_7$) is a commercially available compound that can be easily obtained in the form of a precipitate in a laboratory by simply mixing up two aqueous solutions—$AgNO_3$ and TSC ($Na_3C_6H_5O_7$) (Eq. (1)).

$$3AgNO_3(aq) + Na_3C_6H_5O_7(aq) \rightarrow Ag_3C_6H_5O_7(s)\downarrow + 3NaNO_3(aq) \quad (1)$$

This reaction is rapid, and white precipitate of Ag-Cit is formed ($K_{sp} = 6.4 \times 10^{-14}$)[13] in the mixture as soon as the two aqueous solutions are mixed (inset of Figure 1(a)). After mixing the two aqueous solutions without stirring (0 rpm), the vial containing mixed solutions is covered with an aluminum foil to eliminate the chance of external light influence, and is placed on an experimental bench without any perturbation for 0.5 h. The precipitates were loaded on an Si wafer, and their morphology was investigated by SEM (Figure 1(a)). The precipitates show micron-sized (large) and nano-sized (small) spheroid-like structures (bulk Ag-Cit) with an average dimension of 4.1 ± 1.0 (large) and 1.4 ± 0.2 (small) μm length (ave. 2.7 ± 1.6 μm) and 1.1 ± 0.2 (large) and 0.48 ± 0.08 (small) μm diameter (ave. 0.8 ± 0.4 μm) (Figure S1(a), Supporting Information). The standard deviations at each size were high, which means that the size distribution of bulk Ag-Cit is broad as shown in Figure 1(a).

According to the homogeneous nucleation theory,[21] as the number of nuclei increases, the size of particle decreases at a given concentration of the solute. For nuclei to be formed in mixed solutions ($AgNO_3$ + TSC), Ag^+ ions should encounter with citrate ions. When two solutions ($AgNO_3$, TSC) are mixed with each other under stirring, we can expect that the two solutes are mixed well with each other, resulting in increased probability of the formation of large number of nuclei. For a given concentration of solute, due to the formation of large number of nuclei, the concentration of growth species (Ag^+ and citrate ions) and the size of final product decreased. To decrease the size of bulk Ag-Cit, we introduced mechanical stirring, which can rapidly generate more nuclei in the mixed solutions. The precipitates of Ag-Cit compounds were prepared with stirring at 340 rpm for 0.5 h, and the color of precipitate was white (the inset of Figure 1(b)), which was similar to that prepared without stirring (the inset of Figure 1(a)). However, their microscopic morphology (Figure 1(a) and (b)) was completely different. Ag-Cit compounds prepared with stirring had a morphology similar to rod-like nanostructures (Ag-Cit nanorods), which was completely different from that of bulk Ag-Cit. The length and diameter of Ag-Cit nanorods were 1.3 ± 0.44 and 0.13 ± 0.03 μm, respectively (Figure S1(b)). Comparing them with the variation in the average dimensions of bulk Ag-Cit, the length of Ag-Cit nanorods slightly changed from 2.7 ± 1.6 to 1.3 ± 0.4 μm, whereas the diameter of Ag-Cit nanorods significantly decreased from 0.8 ± 0.4 to 0.13 ± 0.03 μm, resulting in an increase in aspect ratio from 3.4 to 10.0 (Figure S2). It should be noted that there were some slight variations in the average length and diameter of Ag-Cit nanorods, according to the experimental conditions (Figure 1(c) and (d)). For example, when low concentrations of $AgNO_3$ (0.10 M) and TSC (0.10 M) are mixed and stirred at 340 rpm for 0.5 h, the average length and diameter of Ag-Cit nanorods were slightly changed to 0.68 ± 0.19 and 0.11 ± 0.02 μm, respectively (Figures 1 (c) and S1(c)). The dimensions of Ag-Cit nanorods can also be changed by varying the duration of stirring. The length and diameter of Ag-Cit nanorods are decreased to 0.7 ± 0.3 and 0.09 ± 0.02 μm, respectively, when the Ag-Cit nanorods are prepared by prolonged (2 h) stirring (Figures 1(d) and S1(d)). The average length of Ag-Cit nanorods has large variations (0.68–1.3 μm) under different experimental conditions, and large standard deviation (28–43%) in each sample. Because the average diameter of each sample, however, is quite similar (0.09–0.13 μm), and each standard deviation is also small (18–23%), their rod-like structures and aspect ratios are maintained within the concentration range (0.1–0.2 M) and stirring period (0.5–2 h) (Figure S2).

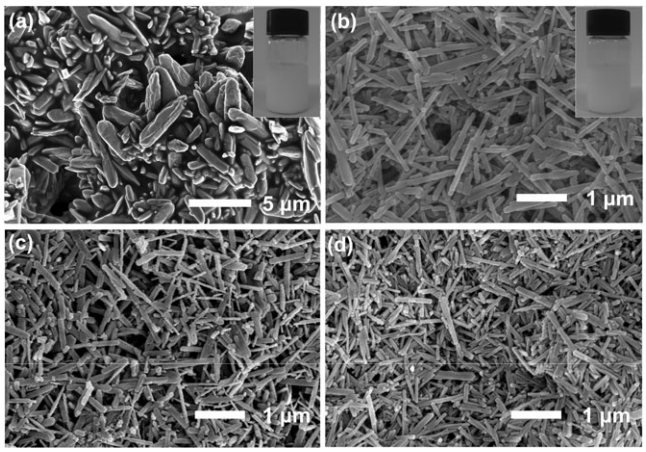

Figure 1. Morphology of Ag-Cit compounds prepared by mixing silver nitrate and trisodium citrate dihydrate solutions at different concentrations (a) 0.2 M and 0.2 M, (b) 0.2 M and 0.2 M, (c) 0.1 M and 0.1 M, and (d) 0.2 M and 0.2 M, and at different stirring rates (a) 0, (b) 340, (c) 340, and (d) 340 rpm for different stirring periods (a) 30, (b) 30, (c) 30, and (d) 120 min, respectively.

As aforementioned, we could explain the size reduction of Ag-Cit compounds by mechanical stirring with homogeneous nucleation theory. The large number of nuclei generated by mechanical stirring hinders excessive growth of seeds, and lead preferentially to smaller crystals with narrow size distribution. On the contrary, the change in shape of Ag-Cit compounds to rod-like nanostructure by mechanical stirring was unexpected. In the following section, we will provide a rough but plausible mechanism for such shape change, or anisotropic growth of crystal, although further experimental data would be needed to verify its mechanism. There have been several research papers regarding the effect of stirring on morphology change of various crystals,[22–25] where anisotropic growth of crystals resulting in the formation of rod-like structures, is demonstrated experimentally and theoretically. These papers explain the anisotropic growth of Ag-Cit compounds and the formation of rod-like structures by mechanical stirring. Crystal growth proceeds through sequential steps (diffusion followed by integration) at diffusion and adsorption layers,

respectively. In diffusion layer (step), solvated species (*e.g.*, Ag^+ or citrate ions surrounded by solvent molecules) diffuse through a concentration gradient from the bulk toward the proximity of the adsorption layer, which forms interfacial region with a thickness of ~1 nm between the surface of crystals and diffusion layer. Reaching the adsorption layer, solvated species are desolvated (removal of their solvent molecules) from Ag-Cit compounds, and then integrated into crystals.[26] Stirring process can introduce liquid flow on exposed facets of crystals in parallel direction with the solid–liquid interfaces, and this liquid flow will generate different shear stresses depending on the intrinsic properties of exposed crystal surfaces (*e.g.*, Miller indices). Thus, environmental conditions of diffusion or adsorption layers would be different and crystal grows asymmetrically at different facets, resulting in Ag-Cit rod-like nanostructures.[27]

To confirm the chemical composition of the precipitates prepared with or without stirring, FT-IR spectroscopy was employed (blue or red line in Figure 2(a), respectively). Both the spectra were obtained in the solid state using KBr pellet method, and showed identical characteristic peaks corresponding to traditional Ag-Cit compounds at 1600, 1400, 1100, and 500 cm^{-1}. A strong band that appeared at 1600 and 1400 cm^{-1} should be designated as asymmetric and symmetric stretching of carboxylate of Ag-Cit compounds, respectively. Because of the resonance effect of carboxylate, double bond character between carbon and oxygen is partially lost resulting in a red shift from the original carbonyl peak positions (~1700 cm^{-1}). A strong band positioned at 1110 cm^{-1} can be assigned as C—O stretching in C—OH. Because Ag-Cit compounds are a third alcohol, the vibrational peak of C—O is shifted to the low energy region from 1200 cm^{-1}, which is the characteristic peak position of C—O stretching in first alcohol. The vibrational peak appeared at low frequency, 500 cm^{-1}, due to Ag—O stretching. The atomic mass of Ag is heavier than that of C, and thus vibrational frequency of Ag—O is lower than that of C—O. For further confirmation, we compared both IR spectra with that of commercially obtained Ag-Cit compounds (black line in Figure 2), and the three spectra are exactly the same, which means that the precipitates prepared with or without stirring are composed of Ag-Cit compounds.

IR spectroscopy is a powerful tool for detecting functional groups of molecules, and we successfully revealed that the chemical structure of both the precipitates is Ag-Cit compounds by comparing the IR spectra of three compounds; however, we did not investigate their crystalline structure. Thus, we employed XRD to compare crystalline phase of the three compounds. The blue or red line in Figure 2(b) is XRD spectrum for precipitates prepared with and without stirring, respectively. The peak positions and relative intensities of both spectra are exactly same, implying that both the precipitates are composed of the same crystalline structure. These two spectra are also compared

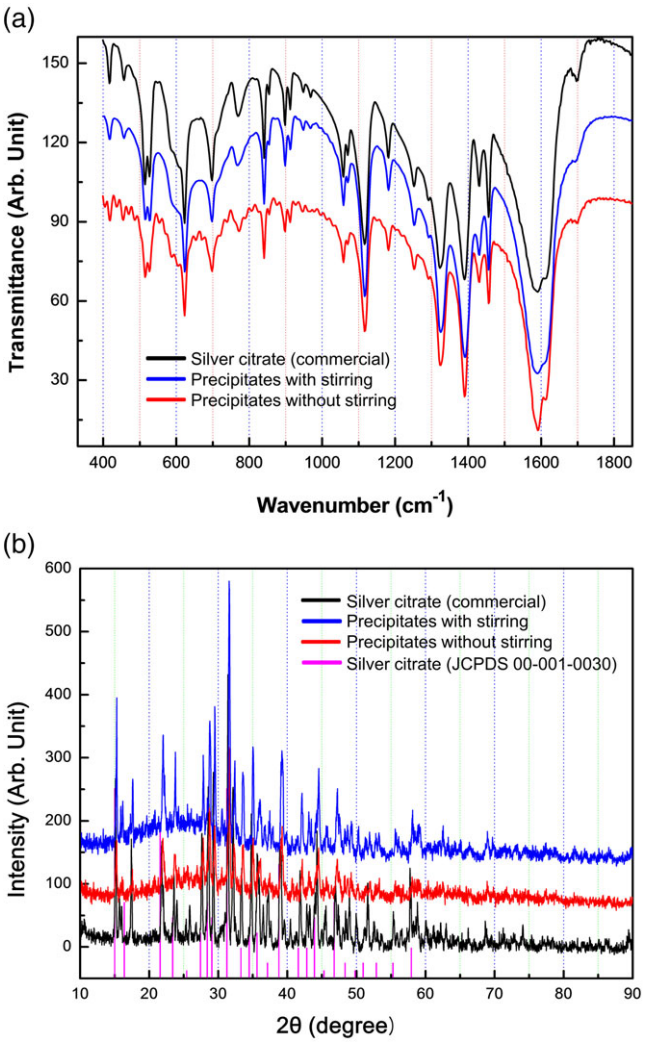

Figure 2. (a) IR spectra for commercially obtained Ag-Cit compounds (black), prepared by stirring (blue), and without stirring (red). All spectra are in good agreement, which means that the three compounds are chemically identical. (b) XRD patterns of commercially obtained Ag-Cit compounds (black), prepared by stirring (blue), and without stirring (red) are compared with those of standard Ag-Cit (pink) (JCPDS 001-0030).

with the spectrum (black line in Figure 2(b)) of commercially purchased Ag-Cit compounds. Relative intensities of the three spectra coincide and their peak positions appear to be at the same diffracted angles. In conclusion, three compounds are composed of the same crystalline phase. We also compared three XRD spectra for the three compounds with 2θ values in JCPDS files of silver citrate (JCPDS 001-0030) (pink bars in Figure 2), and found that most of the peaks of the three spectra, but not all, are equal to the reference values. It can be concluded that the three compounds are Ag-Cit compounds with the same crystalline phase, but they have a slightly different crystalline structure from that of the reference (JCPDS 001-0030). This difference is not resulted from incomplete exchange of silver ions in sodium citrate because the sodium was not detected in energy-

dispersive spectrum of Ag-Cit nanorods (Figure S3). In addition, the thermal gravimetric analysis of Ag-Cit nanorods shows 36% loss in mass, which corresponds to the residual percentage of 63% for theoretical Ag content. These data confirm that sodium ions in sodium citrate are fully exchanged with silver ions, and Ag-Cit nanorods are formed.

It is well known that the ratio of surface area to volume of particles is increased, as the size of particles is decreased. The surface area per volume of Ag-Cit nanorods (33 μm^{-1}) is 3–24 times larger than that of bulk Ag-Cit (9.8 μm^{-1} for small, 1.4 μm^{-1} for large). As the concentration of ions (Ag^+ or citrate ion) released from Ag-Cit compounds, which have biocidal activity, is proportional to the contact surface area of Ag-Cit compounds, it can be easily anticipated that Ag-Cit nanorods will have a higher antimicrobial activity than that of bulk Ag-Cit as demonstrated for Ag nanoparticles in previous reports.[22–25] To test the antibacterial activities dependent on the surface area per volume of Ag-Cit compounds, we initially assessed the antibacterial activity using a paper-disc diffusion method for a Gram-negative *E. coli*. We loaded different concentrations (0, 0.5, 1, 2, 4, 8, and 16 μg/mL) for both samples (bulk Ag-Cit and Ag-Cit nanorods). As shown in Figure 3 (a), bulk Ag-Cit inhibited bacterial growth at only 16 μg/mL concentration; however, Ag-Cit nanorods showed the inhibitory effects from 4 μg/mL concentration. These preliminary data suggest that the Ag-Cit nanorods display higher antibacterial activity than that of bulk Ag-Cit. To quantitatively assess their antibacterial activities, we measured the MIC values of the samples against three Gram-negative and three Gram-positive bacteria. The results are shown in Table 1. The average MIC values of bulk Ag-Cit were 2.0 μg/mL for the three Gram-negative and 10.0 μg/mL for the three Gram-positive bacteria, respectively. It seems that the Gram-negative bacteria are more susceptible to bulk Ag-Cit than Gram-positive are. Among Gram-positive bacteria, *S. aureus* seems to be relatively resistant to bulk Ag-Cit. Similar to the results of the disc diffusion assay, the results for MIC showed that the Ag-Cit nanorods had a higher inhibitory effect than that of bulk Ag-Cit to both Gram-negative and Gram-positive bacteria. The average MIC values of Ag-Cit nanorods were decreased about 1.5 times for Gram-negative and 1.8 times for Gram-positive bacteria. Figure 3(b) shows that the relative antibacterial activity of Ag-Cit nanorods compared to bulk Ag-Cit, and all bacteria, except for *P. aeruginosa*, is more susceptible to Ag-Cit nanorods up to 3.3 folds. Taken together, the antibacterial experiments clearly suggest that the nanorods enhance the antibacterial activity of the Ag-Cit compounds.

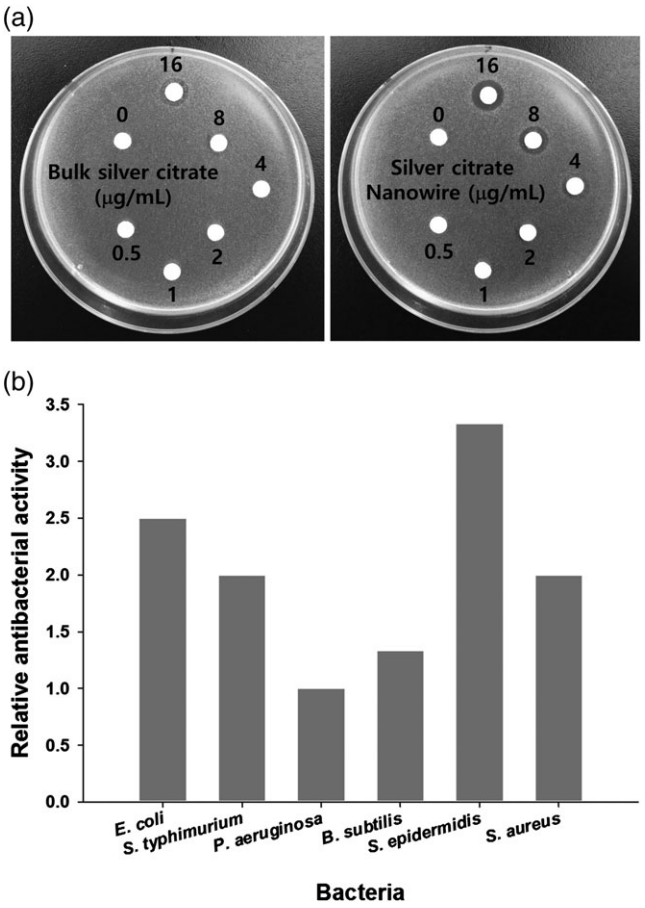

Figure 3. (a) Photographs of the antibacterial test results using the paper-disc diffusion method for bulk Ag-Cit (left) and Ag-Cit nanorods (right) against Gram-negative *E. coli*. (b) The relative antibacterial activities of Ag-Cit nanorods against Gram-negative *E. coli*, *S. typhimurium*, and *P. aeruginosa* and Gram-positive *B. subtilis*, *S. epidermidis*, and *S. aureus*.

Conclusion

In this article, we introduced a facile synthetic method to transform the morphology of Ag-Cit compounds from micron-sized bulk (bulk Ag-Cit) to rod-like nanostructures (Ag-Cit nanorods). This change increased the surface area of Ag-Cit compounds by 3–24 times, and resulted in enhanced antimicrobial activity. Antimicrobial activity of bulk Ag-Cit and Ag-Cit nanorods was investigated against three Gram-negative bacteria (*E. coli*, *S. typhimurium*, and *P. aeruginosa*) and three Gram-positive bacteria (*B. subtilis*, *S. epidermidis*, and *S. aureus*) and were compared with each other. Ag-Cit

Table 1. Summary of minimal inhibitory concentration (μg/mL) against Gram-negative and Gram-positive bacteria.

		Bulk Ag-Cit		Ag-Cit nanorods	
Bacteria		Each	Average	Each	Average
Gram (−)	*E. coli*	2.0	2.0	0.8	1.3
	S. typhimurium	2.0		1.0	
	P. aeruginosa	2.0		2.0	
Gram (+)	*B. subtilis*	8.0	10.0	6.0	5.5
	S. epidermidis	2.0		0.6	
	S. aureus	20.0		10.0	

nanorods exhibited stronger biocidal effect than that exhibited by bulk Ag-Cit by 1.3–3.3 times for most of the bacteria tested, except *P. aeruginosa*.

Acknowledgments. This study was supported by research fund from Chosun University 2013.

Supporting Information. Additional supporting information is available in the online version of this article.

References

1. H. Zhang, M. Wu, A. Sen, In *Nano-Antimicrobials*, N. Cioffi, M. Rai Eds., Springer, New York, **2012**, p. 3.
2. A. D. Russel, W. B. Hugo, In *Progress in Medicinal Chemistry*, G. P. Ellis, D. K. Luscombe Eds., Elsevier Science, Amsterdam, **1994**, p. 351.
3. K. A. Strohfeldt, *Essentials of Inorganic Chemistry*, Wiley, New Jersey, **2014**.
4. J. W. Alexander, *Surg. Infect.* **2009**, *10*, 289.
5. H. J. Klasen, *Burns* **2000**, *26*, 131.
6. R. J. White, R. Cooper, *Wounds* **2005**, *1*, 51.
7. J. Y. Kim, T. Kim, J. Yoon, *J. Korean Ind. Eng. Chem.* **2009**, *20*, 251.
8. H.-J. Park, J. Y. Kim, J. Kim, J.-H. Lee, J.-S. Hahn, M. B. Gu, J. Yoon, *Water Res.* **2009**, *43*, 1027.
9. S. Y. Liau, D. C. Read, W. J. Pugh, J. R. Furr, A. D. Russell, *Lett. Appl. Microbiol.* **1997**, *25*, 279.
10. S. Doores, In *Antimicrobials in Foods*, 2nd ed., P. M. Davidson, A. L. Branen Eds., Marcel Dekker Inc., New York **1993**, p. 95.
11. K. Imai, I. Banno, T. Hjima, *J. Gen. Appl. Microbiol.* **1970**, *16*, 479.
12. C. G. Rammell, *J. Bacteriol.* **1962**, *84*, 1123.
13. S. Djokić, *Bioinorg. Chem. Appl.* **2008**, *2008*, 436458.
14. Silver 100. Ionic silver complex. **2017**. URL http://www.silver100.com (accessed January 23, 2017).
15. Pure Bioscience. Silver dihydrogen citrate. **2017**. URL https://www.purebio.com/technology/silver-dihydrogen-citrate-sdc.htm (accessed January 23, 2017).
16. Laboratorios Argenol. Silver citrate. **2017**. URL http://www.laboratorios-argenol.com/en/products/silver-salts/silver-citrate (accessed January 23, 2017).
17. S. Pal, Y. K. Tak, J. M. Song, *Appl. Environ. Microbiol.* **2007**, *73*, 1712.
18. B. Ajitha, Y. A. K. Reddy, P. S. Reddy, *Powder Technol.* **2015**, *269*, 110.
19. A. Azam, A. S. Ahmed, M. Oves, M. S. Khan, A. Memic, *Int. J. Nanomedicine* **2012**, *7*, 3527.
20. L. M. Gilbertson, E. M. Albalghiti, Z. S. Fishman, F. Perreault, C. Corredor, J. D. Posner, M. Elimelech, L. D. Pfefferle, J. B. Zimmerman, *Environ. Sci. Technol.* **2016**, *50*, 3975.
21. G. Cao, Y. Wang, *Nanostructures and Nanomaterials*, 2nd ed., World Scientific, Singapore, **2011**.
22. M. A. Mahmoud, M. A. El-Sayed, J. Gao, U. Landman, *Nano Lett.* **2013**, *13*, 4739.
23. M. A. García, V. Bouzas, N. Carmona, *Mater. Chem.Phys.* **2011**, *127*, 446.
24. Z. Zhang, Y. Zheng, J. Zhang, Q. Zhang, J. Chen, J. Liu, X. Liang, *Cryst. Growth Des.* **2007**, *7*, 337.
25. M. A. Cheney, P. K. Bhowmik, S. Mortiuchi, M. Villalobos, S. Qian, S. W. Joo, *J. Nanomater.* **2008**, *2008*, 168716.
26. H. J. Scheel, D. Elwell, *J. Electrochem. Soc.* **1973**, *120*, 818.
27. J. Gao, W. D. Luedkte, U. Langman, *Tribol. Lett.* **2000**, *9*, 3.

